Composite Structures 123 (2015) 169–179

Contents lists available at ScienceDirect

Composite Structures

journal homepage: www.elsevier.com/locate/compstruct

Manufacturing and characterization of polyurethane based sandwich composite structures

M. Mohamed [a], S. Anandan [a], Z. Huo [a], V. Birman [a,c], J. Volz [b], K. Chandrashekhara [a,*]

[a] Department of Mechanical and Aerospace Engineering, Missouri University of Science and Technology, Rolla, MO 65409, United States
[b] Department of Civil, Architectural and Environmental Engineering, Missouri University of Science and Technology, Rolla, MO 65409, United States
[c] Engineering Education Center, Missouri University of Science and Technology, Rolla, MO 65409, United States

ARTICLE INFO

Article history:
Available online 26 December 2014

Keywords:
Polyurethane resin
Trapezoid foam
Composite sandwich structure
VARTM

ABSTRACT

Demand has been growing for structural systems utilizing new materials that are more durable and require less maintenance during the service lifetime. In particular, sandwich composite structures attract attention due to many advantages such as light weight, high strength, corrosion resistance, durability and speedy construction. In this study, three designs of glass reinforced composite sandwich structures, namely boxes (web-core W1), trapezoid and polyurethane rigid foam, are fabricated using new generation of two-part thermoset polyurethane resin systems as matrix materials with vacuum assisted resin transfer molding (VARTM) process. The stiffness, load-carrying capacity and compressive strength were evaluated. Core shear, flatwise and edgewise compression tests were carried out for these three models. The mechanical response of three designs of sandwich structures under flexural loading were analyzed using commercial finite element method (FEM) software ABAQUS. The simulation results of flexural behavior were validated by experimental findings.

1. Introduction

Composite sandwich structures are increasingly used in civil infrastructures due to their many advantages such as light weight, high stiffness to weight ratio, corrosion resistance, good fatigue resistance and high durability. The main advantage of a sandwich construction in civil engineering applications is its ability to provide increased flexural strength without a significant increase in weight.

With the development of composite manufacturing processes, such as resin transfer molding (RTM), pultrusion and VARTM, sandwich structures fabricated using polymer matrix composites have been explored since early 1980s. In particular, VARTM is a low-cost composite manufacturing process that has been employed to manufacture various large components including turbine blades, boats, rail cars and bridge decks [1,2].

Out of many applications of sandwich composite structures in civil infrastructures, using sandwich composite materials in civil infrastructures to replace the conventional materials significantly reduces dead load. Furthermore, in new constructions, lower dead load can translate into savings throughout the structure, as the size of structural members and foundation is reduced accordingly. The other reason for the use of composite materials is their higher corrosion resistance [3].

The necessity to study the structural behavior and failure characteristics of sandwich structures has increased during recent years. Recent applications have demonstrated that fiber reinforced composite sandwich construction can be effectively and economically used in the civil infrastructure and several critical weight applications. A combination of good flexural and compressive strength coupled with high weight savings is critical in these applications. A number of research papers have been presented on experimental and numerical investigation on the mechanical behavior of sandwich composites.

Manalo et al. [4] investigated the flexural behavior of a new generation composite sandwich beams made up of glass fiber reinforced polymer facesheet and modified phenolic core material experimentally and numerically. The results showed that the composite sandwich beams tested in the edgewise position failed at a higher load with less deflection compared to specimens tested in the flatwise position. Finally, the result of the study showed the high potential of this innovative composite sandwich panel for structural laminated beam. Dai et al. [5] investigated the failure behavior of sandwich beams manufactured using VARTM process in static 3-point and in 4-point bending using two different core

* Corresponding author. Tel.: +1 573 341 4587.
E-mail address: chandra@mst.edu (K. Chandrashekhara).

http://dx.doi.org/10.1016/j.compstruct.2014.12.042
0263-8223/

materials. The results showed long beams failed in the face on the tension side when the tensile strength of the face was exceeded. The wood core was predicted to fail laterally in the thickness direction before the face failure because of the relatively high tensile stress in the core. Reisa et al. [6] studied the delamination problems typically faced in traditional glass fiber reinforced polymer (GFRP) sandwich panels. The influence of the panel thickness, through-thickness fiber configuration and density, and other parameters on the tension, compression, flexure and shear behavior of the panels were discussed. The results showed the behavior of the face sheets under tension is bi-linear which could be caused by the presence of the fibers in the perpendicular direction.

A series of analytical and experimental investigations is presented to study the response and failure of truss core sandwich panels. Xiong et al. [7] studied the response of carbon fiber composite pyramidal truss core sandwich panels subjected to axial compression using analytical models and experiments. The results show after initial peak load, the bond strength was one of the main factors in the performance of the panels. Debonding between the facesheet and core were observed, leading to reduction in the load carrying capacity of the structure. The measured peak loads obtained in the experiments showed good agreement with the analytical predictions. Humpreys et al. [8] studied the structural behavior of monocoque fiber composite truss joints. The joints were subjected to static loading of the diagonal tension member. From the results presented, it can be seen that strong monocoque fiber composite trusses can be produced. Canning et al. [9] proposed a hybrid box section consisting of glass fiber reinforced polymer pultruded box with an upper layer of concrete in the compression side. Cartie and Fleck [10] studied the effects of titanium and carbon fiber pins inserted into the polymethacrylimide foam core of a sandwich panel (with carbon fiber face sheets) in order to increase the through-thickness strength. The results show that the compressive strength is governed by elastic buckling of the pins, with the foam core behaving as an elastic Winkler foundation in supporting the pins. The peak strength of the pin-reinforced core is increased. Aref and Alampalli [11] conducted field tests and studied the dynamic response of the first FRP composite bridge built in USA. The same authors also developed a finite element model using MSC-PATRAN and analyzed the dynamic behavior using ABAQUS. The results indicated that the longitudinal joint is performing as intended, and only high degradation of the joint can be detected using the measured vibration characteristic of the sandwich bridge deck.

Presently, limited literature is available on the mechanical properties of VARTM thermoset PU sandwich structures. In this study, the main objective is performance evaluation of thermoset polyurethane sandwich structure manufactured with low cost VARTM process. The failure mechanisms of VARTM thermoset polyurethane (PU) composite sandwich beams were studied. Three different models of all-fiber reinforced polymer composite sandwich structures utilizing various core designs, namely box, trapezoid and polyurethane (PU) rectangular rigid foam, were fabricated using VARTM process. Woven glass fiber and new generation of two-part thermoset polyurethane resin systems were used for fabrication. Core shear, flatwise compression and edgewise compression tests were performed accordance to ASTM standards C393, C365 and C364 respectively. In addition, finite element analysis was conducted to model the flexural behavior for all three types of sandwich structures.

2. Materials

Three different models were constructed with woven E-glass fiber face sheets. The E-glass fiber, obtained from Owens Corning, OH, was compatible with PU resin. A new generation two-part thermoset polyurethane resin system from Bayer MaterialScience was used as the matrix material. The two-part thermoset resin system (RTM NB #840871) consists of two components. The "A" component is Isocyanate NB#840859 ISO, Diphenylmethane Diisocyanate (MDI-Aromatic). The "B" component is a Polyol (RTM NB#840871), of low viscosity (approx. 350 cPs). The components react rapidly after mixing, forming a highly cross-linked thermoset with good mechanical properties.

Three different materials comprised the sandwich's foam core.

- Type-1: high density (6 lb/ft^3) PU rigid foam with closed cell (Fig. 1a).
- Type-2: low density (2 lb/ft^3) polyurethane foam of a trapezoid shape (Prisma) with a combination of two plies and a knitted E-glass biaxial (+/−45°) matted reinforcement encompassing a single cell (Fig. 1b).
- Type-3: web-core boxes with a low density (2 lb/ft^3) polyurethane foam and matted reinforcement. It had one additional layer mesh mat of glass fiber between each cell of the core (Fig. 1c). The core cells had grooves on their sides to facilitate resin flow across shear webs.

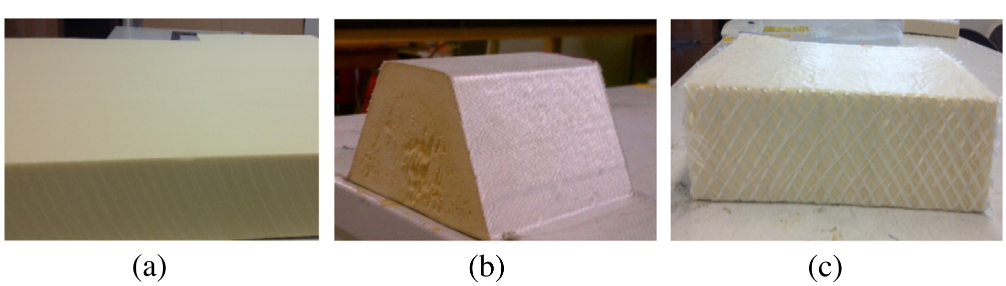

Fig. 1. Three types of foam cores. (a) Type-1 high density PU foam, (b) Type-2 trapezoidal low density foam with mat reinforcement, (c) Type-3 web-core foam with mat reinforcement.

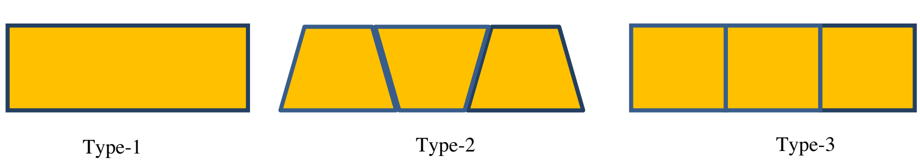

Fig. 2. Sandwich structure models.

3. Experiments

3.1. Manufacturing sandwich composites using VARTM

Three sandwich designs considered in this study are depicted in Fig. 2 that illustrates the model sections for the rectangular PU rigid foam, trapezoid shape profile and boxes. Sandwich specimens with E-glass/PU face sheets were manufactured at Missouri S&T composites lab. VARTM, a cost-effective method, was used to fabricate small to large size FRP composite systems. The overall depth was fixed at 54.61 mm (2.15 in.). Each face sheet consisted of three layers of woven E-glass fibers.

Three shear layers (E-BXM1715-10) were added during the manufacturing process to the Type-2 model between the trapezoidal sections. The resin was initially cured at room temperature for 6 h followed by 70 °C for 1 h. It was then post-cured at 80 °C for 4 h. Fig. 3 illustrates the fabrication of specimens using VARTM process. Two panels of dimensions, 914.4 mm × 304.8 mm × 54.61 mm (36 in. × 12 in. × 2.15 in.), were manufactured for each design. The dimensions of test specimens are listed in Table 1. In the present work, five specimens of each type were tested for the corresponding tests.

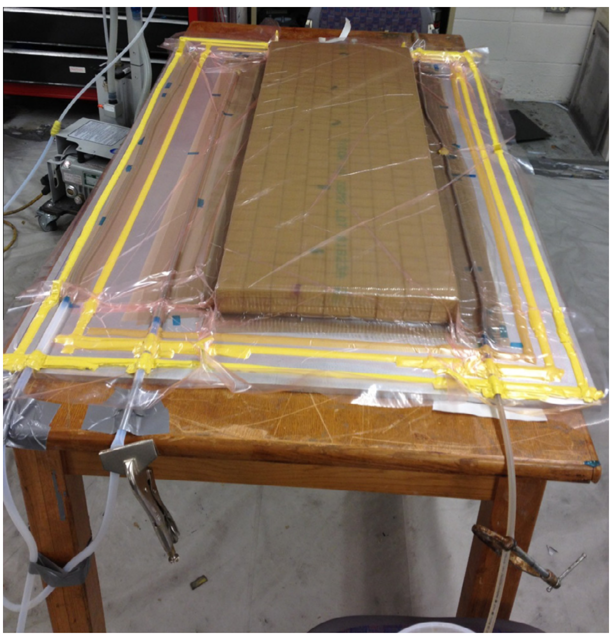

Fig. 3. VARTM setup for sandwich composite.

3.2. Core shear properties of sandwich constructions by beam flexure test

The tests of simply supported panels were conducted in accordance with ASTM C-393. The length of the support span was equal to 203.2 mm (8 in.). An Instron 5985 test machine with a 250 kN load cell was used to apply load to the sandwich specimen at a constant crosshead speed of 6 mm/min (0.25 in/min). Both the location and type of failure were recorded. Core shear stress at failure, as well as stiffness, were calculated from the resulting load versus deflection curve and the core specimen dimensions.

3.3. Flatwise compression test

Flatwise tests were performed according to ASTM standard C365M–11. The differences in compressive strengths and elastic moduli of sandwich cores in the direction normal to the plane of the structure between three analyzed designs were investigated. Tests were performed on an Instron-5985 testing machine with a 250 kN load cell at a rate of 2 mm/min (0.079 in/min). Bitzer [12] found that neither the compressive properties nor the shear moduli vary much as the thickness changes, while the shear strength reduces as the thickness increases.

3.4. Edgewise compression test

The edgewise compressive strength of short sandwich construction samples is important as it provides the basis for the assessment of the load-carrying capacity. Edgewise compression tests of the sandwich structure models were performed on an Instron 5985 machine in accordance with ASTM C364. Compression was applied at a crosshead speed of 10 mm/min (0.39 in/min) using an edgewise compression test fixture. Attention was paid to make sure the ends of the specimen are flat to prevent localized end failures.

Table 1
Test specimen specifications.

Test	Specimen model type	Facesheet constituents	Dimensions		
			Length mm (in.)	Width mm (in.)	Thickness mm (in.)
Flexure	Type-1	E-glass/PU	254 (10)	74.93 (2.95)	54.61 (2.15)
	Type-2	E-glass/PU	254 (10)	74.93 (2.95)	54.61 (2.15)
	Type-3	E-glass/PU	254 (10)	74.93 (2.95)	54.61 (2.15)
Flatwise compression	Type-1	E-glass/PU	44.45 (1.75)	50.8 (2)	54.61 (2.15)
	Type-2	E-glass/PU	44.45 (1.75)	54.61 (2.15)	54.61 (2.15)
	Type-3	E-glass/PU	44.45 (1.75)	50.8 (2)	54.61 (2.15)
Edgewise compression	Type-1	E-glass/PU	203.2 (8)	101.6 (4)	54.61 (2.15)
	Type-2	E-glass/PU	203.2 (8)	101.6 (4)	54.61 (2.15)
	Type-3	E-glass/PU	203.2 (8)	101.6 (4)	54.61 (2.15)

Table 2
Core shear test results.

Specimen model type	Flexural strength (MPa)	Flexural failure strain (%)	Maximum load (N)	Facing ultimate stress (MPa)	Core shear stress (MPa)
Type-1	6.10 ± 0.4	0.19 ± 0.02	4477.91 ± 112	22.84 ± 1.2	0.57 ± 0.2
Type-2	21.52 ± 1.1	0.16 ± 0.04	16371.16 ± 110	41.78 ± 1.6	2.02 ± 0.6
Type-3	6.41 ± 0.8	0.07 ± 0.01	4708.26 ± 89	27.67 ± 1.4	0.60 ± 0.1

4. Results and discussion

4.1. Core shear test

4.1.1. Comparison of core shear strengths

Core shear tests were conducted on the three fabricated sandwich models. The failure loads of the sandwich models, Type-1, Type-2 and Type-3, were 4100 N, 16300 N and 5200 N, respectively. As expected, the gain in strength in the Type-2 model was quite significant due to the shear layers implanted during the manufacturing between the trapezoid sections.

Type-1 models exhibited maximum deflection because of the foam compaction under loading. Unlike Type-2 and Type-3 models, this model does not have stiffeners that explain its relatively low stiffness. The experimental data is presented in Table 2 reflecting that Type-2 models carried significantly higher loads than the other models.

Fig. 4 depicts the flexural stress–strain curve for the three sandwich structure models. The trapezoid shaped foam Type-2 model had a flexural strength four times higher than the other sandwich structure models. Due to the E-glass shear webs used in the trapezoid design, both the apparent shear modulus of and the ductility for the flexural failure response increased.

4.1.2. Core shear stress and facing stress

In sandwich structures, the core absorbs the shear load while the facesheets carry the bulk of the bending load. Both the core and facesheets were considered for composite sandwich beams tested in this study. Both the core shear stress (τ) and the facesheet bending stress (σ) values were calculated using the equations given in the ASTM C 393-94. In the following, Eq. (1) was used to calculate the maximum core's shear stress (τ) for all types of bending tests. Eq. (2) was used to calculate the facing stress (σ) for three-point bending test.

$$\tau = \frac{F}{(d+c)b} \tag{1}$$

$$\sigma = \frac{FL}{2(d+c)tb} \tag{2}$$

where F is the maximum force prior to failure, L is the span length, b is the sandwich width and d, c and t represent the thickness of the sandwich, core and facesheet, respectively.

It is interesting to note that the response of the panel with unreinforced foam core (Type-1) reflects the behavior of closed-cell foams subject to uniaxial compression discussed by Gibson and Ashby [13]. The initial elastic response is followed with a nearly horizontal section of the stress–strain or load–deflection curve. This section corresponds to buckling and crushing of the cell walls. In pure foam specimens such behavior is followed with a densification phase of response as the load increases. In sandwich panels the latter phase is missing due to failure of the entire structure. While the foam response described above is characteristic for uniaxial compression, apparently, the same features are present in the case of transverse shear loading of the core of a sandwich structure.

4.1.3. Effect of flexural stiffness (ϕ)

The facesheet tensile modulus obtained from previous studies for the web-core and PU rectangular models was 19,534.00 MPa [14]. The tensile modulus of the shear layers of the Type-2 model was 14,344.65 MPa. It was obtained from the tensile test performed on the shear layers according to ASTM D3039. The effective flexural moduli of the PU rigid foam, prisma foams and web-core were 8.27 MPa, 4.41 MPa and 4.48 MPa respectively. These values were obtained from the manufacturing data sheet. As anticipated, the elastic modulus of facesheet is significantly higher compared to the elastic modulus of core.

4.1.4. Effect of stiffener and stitching orientation

The strength of a sandwich structure is a function of several factors including the properties of the materials used and the geometry of the structures. Strength of the bond between the layers is also important. In case of Type-2 and Type-3 the foam effect was ignored because the foam's elastic compressive modulus was

Table 3
Flatwise test results.

Specimen model type	Maximum load (N)	Ultimate flatwise compressive stress (MPa)	Failure compressive strain (%)	Deflections (mm)
Type-1	2357.54 ± 131	1.21 ± 0.1	0.38 ± 0.05	21.29 ± 3
Type-2	9230.53 ± 157	3.81 ± 0.2	0.09 ± 0.02	6.03 ± 0.8
Type-3	5477.19 ± 95	2.82 ± 0.2	0.22 ± 0.01	12.02 ± 2

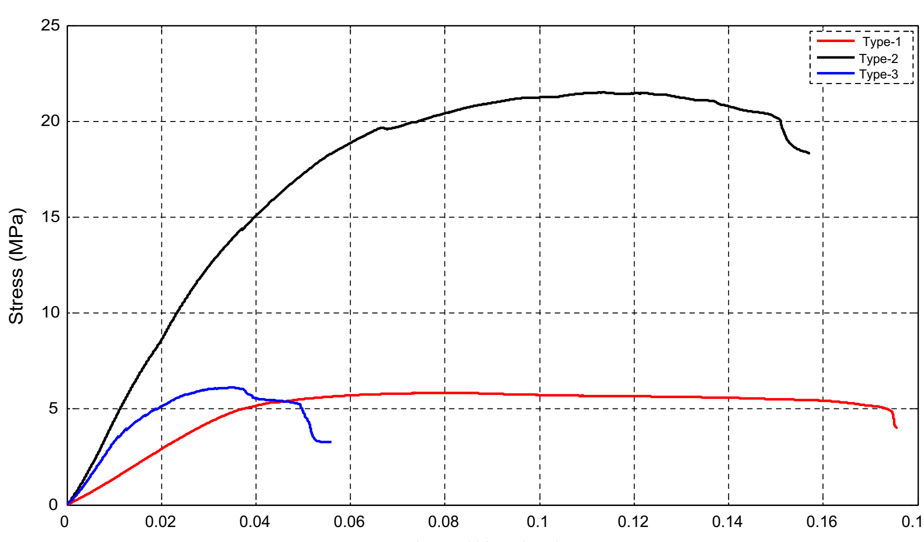

Fig. 4. Stress vs. strain at mid-span curve generated in the core shear test.

approximately 0.01% from the compressive modulus of the facing glass fiber and web layers. Three different configurations for sandwich panel has shown a significant variance in load carry values as well as bending load as shown in Fig. 4. It has been found that the Type-2 have shear layers combination of two plies and a knitted E-glass biaxial (+/−45°) matted reinforcement produced highest bending load in comparison to Type-3 stitched and Type-1 unstitched foam.

The sample exhibited characteristics typical of stiffened sandwich cores including: elastic behavior during initial loading and increasing load support capability until the peak strength was reached. This is attributed to additional support provided by the shear layers embedded between the form cells in Type-2. In addition, these plies contributions are depended on orientation. In case of (±45°) oriented plies this leads to transfer the load from the facing through these shear layers, also lead to higher flexural strength and higher shear strength. For the Type-2 the thin stiffener layer has less load carrying capability compared to (±45°) oriented plies.

An important structural property that affects flexural stiffness is the length or loading span. The flexural stiffness is inversely proportional to the length. The modulus of elasticity also influences the flexural stiffness [15]. The functional relationship between

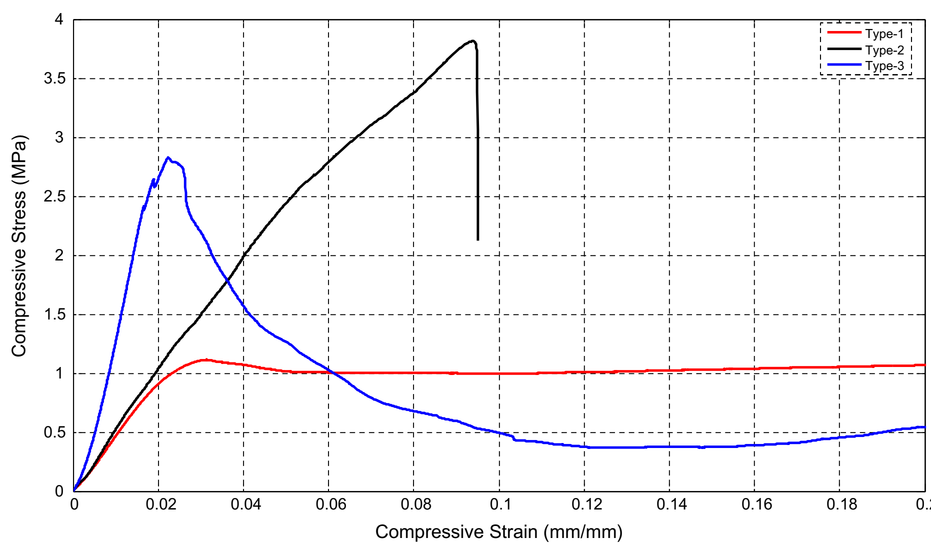

Fig. 5. Stress vs. strain curve in flatwise compression test.

Fig. 6a. Samples Type-1 during flatwise compression test.

Fig. 6b. Samples Type-2 during flatwise compression test.

Fig. 6c. Samples Type-3 during flatwise compression test.

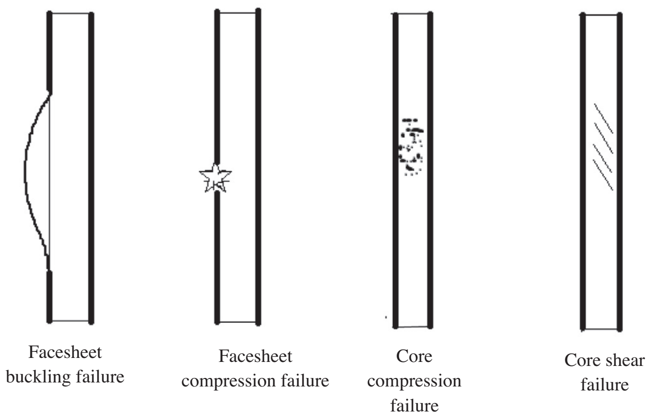

Fig. 7. Failure modes of sandwich structures under edgewise compression test.

the flexural stiffness of the specimen, modulus of elasticity and length is given by Eq. (3):

$$\phi \propto E/l^3 \tag{3}$$

4.2. Flatwise compression test

Flatwise compression tests were performed on the sandwich structure models to investigate differences in strength and modulus for various core types. Five specimens from each category were tested according to ASTM standard C365M. The flatwise compressive strength was calculated using Eq. (4) according to ASTM C365M standard:

$$F_c = P_{max}/A \tag{4}$$

where F_c is the ultimate flatwise compressive strength (MPa), P_{max} is the ultimate force prior to failure (N) and A is the area of the of the surface of facing subjected to compressive load (mm^2).

The average nominal compressive strength and the displacement of Type-1, Type-2, and Type-3 models respectively are listed in Table 3. From experimental data, it is observed that for equal core thickness, flatwise compressive strength of Type-2 model is higher than those of Type-1 and Type-3 counterparts due to the strengthening effect of shear layers between the foam cells. The peak compressive load of the Type-2 model was nearly five times higher than that of Type-1 and two times higher than that of Type-3.

The first part of the compressive stress–strain curve (Fig. 5) is linear elastic until the stress reaches a maximum for the three models. At this point, the structure begins to fail. In case of Type-1 model, a flat region is observed because of the foam compaction associated with buckling of cell walls described above. In Type-2 and Type-3 models the load drops rapidly due to failure of the stiffening layers. This result is comparable to the observations of Corigliano et al. [16]. The overall behavior of Type-2 model is governed by the shear layers that behave similar to plates on elastic foundation provided by foam. The postbuckling response of plates being stable, the response is characterized by ascending stress–strain curves until collapse. The response is somewhat different in Type-3 model where both the web and facesheet are subject to a larger compressive stress under the same load than shear layers in Type-2 model. Although the region of postbuckling web response is detectable, it is much "smaller" and failure occurs at a smaller applied force. It was also noted that adding stitches in the transverse direction to Type-3 model, increases its mechanical

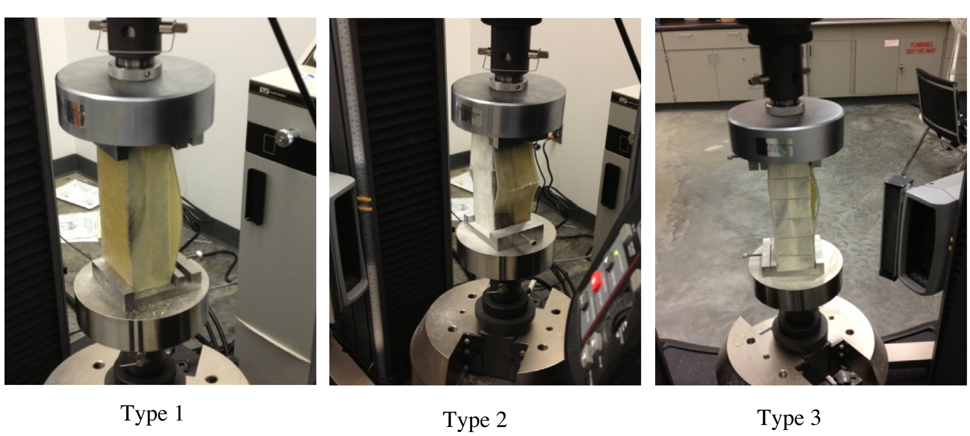

Fig. 8. Crushing configurations of the three models under edgewise compression test.

performance. The difference between failure of Type-1, Type-2 and Type-3 models is observed in Figs. 6a–6c where the compaction in the case of Type-1 is evidently different from the failure associated with buckling of web in Type-3 model.

4.3. Edgewise compression test

Both the compressive properties and the failure behavior of the sandwich model specimens were analyzed in the course of an in-plane edgewise compressive load. Fig. 7 illustrates the deformation and failure of the tested specimens under edgewise compression test. Specimen failure can take place according to several modes of failure [17]. The overall crushing configurations corresponding to each mode are shown in Fig. 8.

- Mode I: buckling of facesheet.
- Mode II: progressive end-crushing of the sandwich facesheet.
- Mode III: core compression failure.
- Mode IV: core shear failure.

The load–displacement curves obtained from the edgewise compression tests conducted on the sandwich structure models are depicted in Fig. 9. Experimental results and failure mode identification are listed in Table 4.

The mode I failure (buckling of facesheets) of Type-1 model began at the end of a linear elastic compression phase when the applied load (P) reached a critical value (29,223.51 N). Debonding was observed at the facesheet-to-core interface upon the onset of facesheet buckling. A thin layer of the foam core remained on the debonded facesheet laminates (Fig. 10a) suggesting that debonding could actually be associated with fracture throughout the core propagating close to the interface with the facesheet. This debonding caused a drop in the compressive load followed with the ultimate failure.

In case of Type-2 model, the facesheet initially buckled under compressive load. Buckling was followed with failure of the bond between the foam core and the facing sheet (Fig. 10b). Subsequently, as the buckling zone of the facesheets expanded, extensive cracking and delamination occurred between the layers accompanied by debonding of the core-facesheet interface (Fig. 10b). The shear layer reinforcement resulted in a significant increase in the edgewise compression strength of the panels reaching 138.55 MPa. This is significantly greater than the compressive strength of Type-1 and Type-3 panels (Table 4).

Table 4
Edgewise compression test results.

Specimen model type	Maximum load (N)	Ultimate edgewise compressive stress (MPa)	Deflection (mm)	Failure mode
Type-1	29223.51 ± 126	76.40 ± 2.3	6.49	I
Type-2	102050.34 ± 171	138.55 ± 1.4	10.26	I,II
Type-3	20670.24 ± 104	62.37 ± 2.1	3.01	I

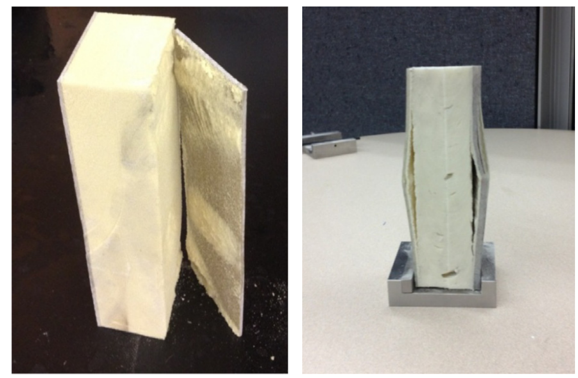

Fig. 10. (a) Facesheet debonding of Type-1 model, (b) failure of Type-2 model.

Mode I failure was exhibited by Type-3 models. The thin stiffness layer between the cells of the core resists buckling during the test (Fig. 11). A sudden drop in the compressive load after the initial peak of the force–displacement curve is attributed to failure of the stiffener layers. The critical load, P_{max}, for buckling of the facesheet laminates was smaller than that recorded for Type-1 model that failed in mode I.

Facing compressive stress, defined in the ASTM standard C364 as the ratio of the peak load (P_{max}) to the loaded face area, is calculated using Eq. (5):

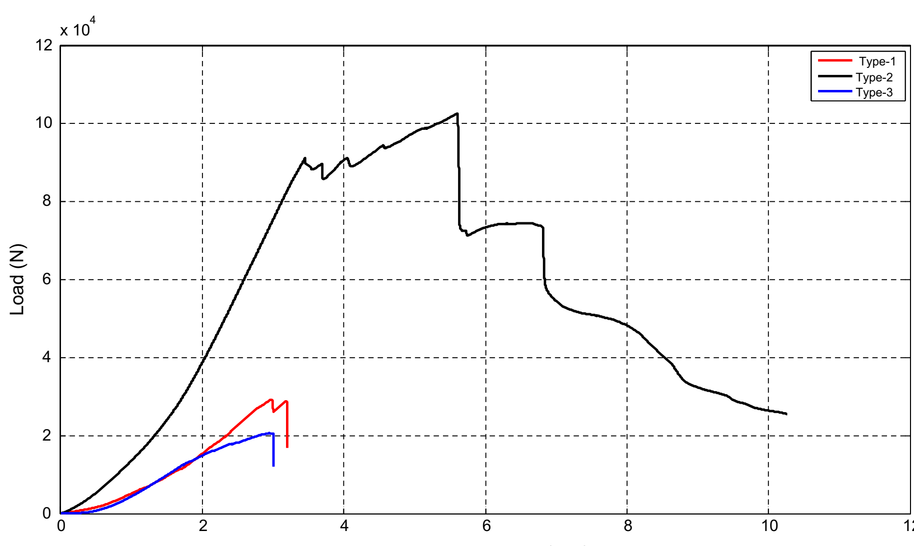

Fig. 9. Load–displacement curves from the edgewise compression test.

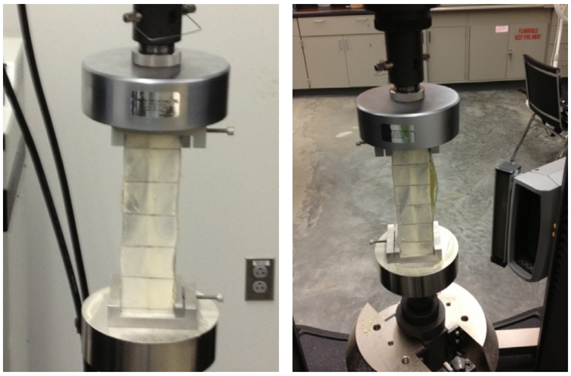

Before the failure After the failure

Fig. 11. Type-3 model before and after failure under edgewise compression test.

$$\sigma = \frac{P_{max}}{[b(2 \times t_f)]} \tag{5}$$

where σ is the ultimate edgewise compressive strength (MPa), P_{max} is the ultimate force prior to failure (N), b is the width of specimen(mm), and t_f is the thickness of a single facesheet (mm).

4.4. Finite element analysis

A quasi-static three-dimensional model has been developed to simulate the mechanical behavior for three types of sandwich structures under flexural loading. Geometries of three types of sandwich structures are shown in Fig. 12. All three types of a sandwich structures consist of three-layer top and bottom woven E-glass/polyurethane facesheets. The foam core for Type-1 sandwich structure is high density polyurethane foam. Type-2 sandwich structure consists of trapezoidal low density foam with mat reinforcement represented by three shear layers of E-BXM1715-10 embedded between trapezoidal sections. Type-3 sandwich structure consists of low density foam embedded with distributed one-layer vertical mat stiffener. To reduce the computational cost, half of overall structure is modeled utilizing symmetry along

Table 5
Mechanical properties of woven E-glass/polyurethane and foams.

Material	Property	Value
Woven E-glass/polyurethane	Longitudinal modulus, E_x (GPa)	19.5
	Transverse modulus, E_y (GPa)	19.5
	Poisson's ratio, υ	0.13*
	In-plane shear modulus, G_{12} (GPa)	5.5*
	Out-plane shear modulus, G_{13} (GPa)	5.1*
	Out-plane shear modulus, G_{23} (GPa)	5.1*
High density polyurethane foam	Compressive modulus, E (MPa)	30
	Poisson's ratio, υ	0.3
	Compressive strength, σ_t (MPa)	1.04
Low density polyurethane foam	Compressive modulus, E (MPa)	2.83
	Poisson's ratio, υ	0.3
	Compressive strength, σ_t (kPa)	117

Properties with '*' are approximated or obtained from literatures, others are from experiments.

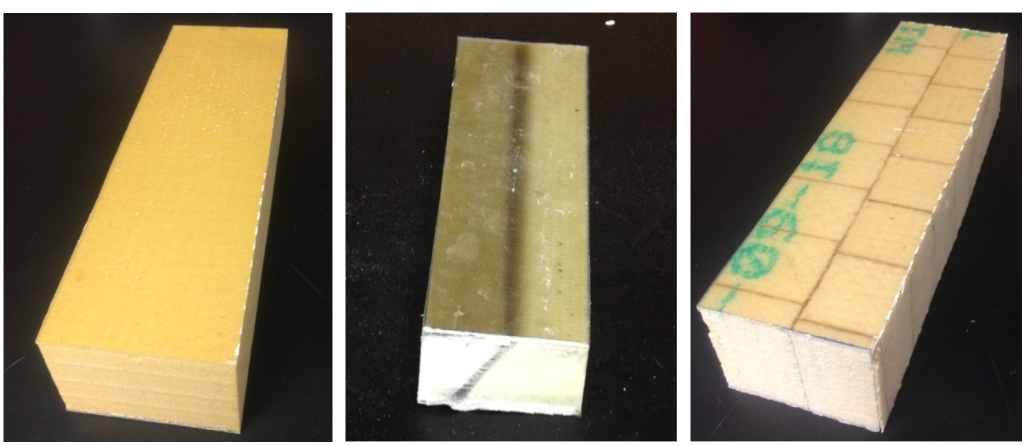

(a) (b) (c)

Fig. 12. Geometry of three types of sandwich samples, (a) Type-1, (b) Type-2, (c) Type-3.

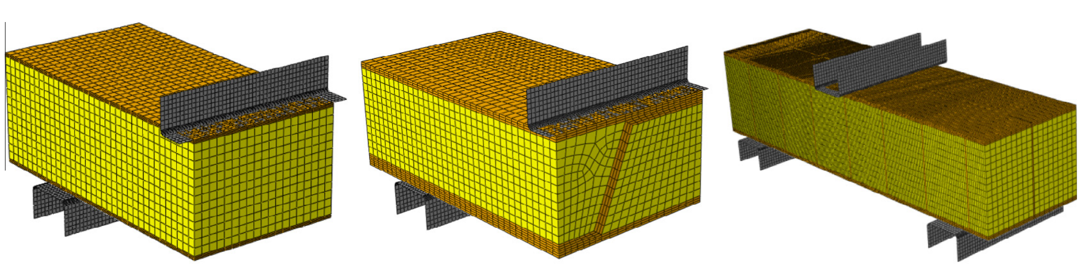

(a) (b) (c)

Fig. 13. Finite element meshing for three types of sandwich structure assemblies, Type-1, (b) Type-2, (c) Type-3.

length direction for Type-1 and Type-2 sandwich structures, and a full modeling is adopted for Type-3 sandwich structure due to its asymmetric distribution of vertical stiffener. The finite element meshing for three types of sandwich structures are shown in Fig. 13.

In all three cases, top and bottom facesheets are meshed using three-layer 8-node quadrilateral reduced-integration continuum shell elements. In the case of Type-2 sandwich structure, the shear mat reinforcements are meshed using 8-node linear reduced-integration hexahedral elements. The mechanical properties of woven E-glass/polyurethane are listed in Table 5. In all three cases, both high density polyurethane foam and low density foam are meshed using 8-node linear reduced-integration hexahedral elements. The compressive stress–strain curve for high density polyurethane foam is shown in Fig. 14, which presents three distinct stages: a linear elastic stage at low stresses, followed by a collapse plateau corresponding to progressive crushing at a nearly constant stress level, and then followed by a densification region in which the stress rises steeply. The mechanical properties of high density polyurethane foam and low density foam are listed in the Table 5. The steel loading head and supports were modeled using rigid four-node bilinear shells elements. When applying the boundary conditions, both left and right supports were fully constrained. For steel loading head, all degrees of freedom, except for the displacement along Z direction, were constrained. Also in the case of Type-1 and Type-2 sandwich structures, symmetric boundary conditions are applied on the symmetric surface. Hard contact property in the normal direction is applied in the interaction between loading head/top facesheet, and supports/bottom facesheet. Displacement loading is applied on the steel punch.

In this study, nonlinear finite element analysis was conducted considering the combined effects of the linear elastic behavior of laminates and the nonlinear behavior of foam core, and only the initial part of mechanical response before ultimate failure under

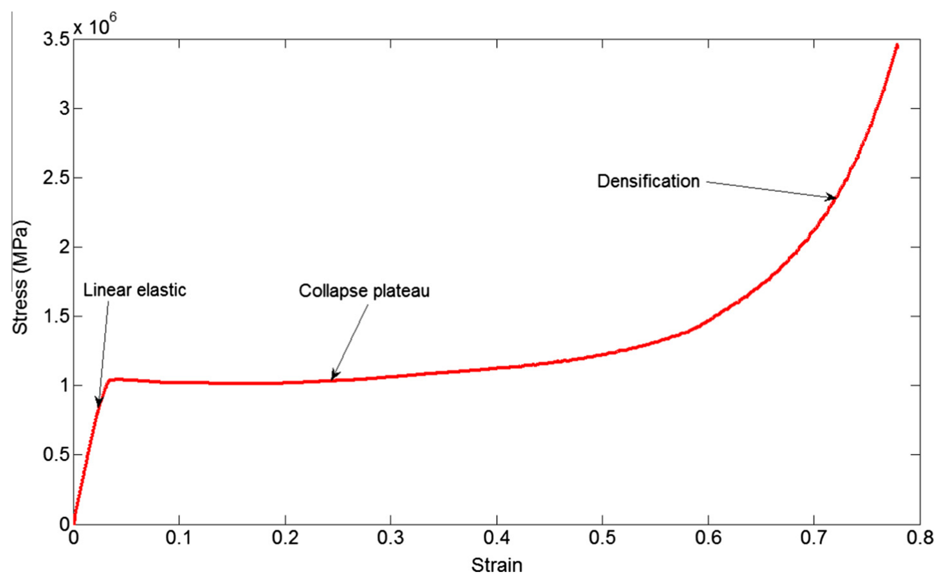

Fig. 14. Compressive strain–stress curve for high density polyurethane foam.

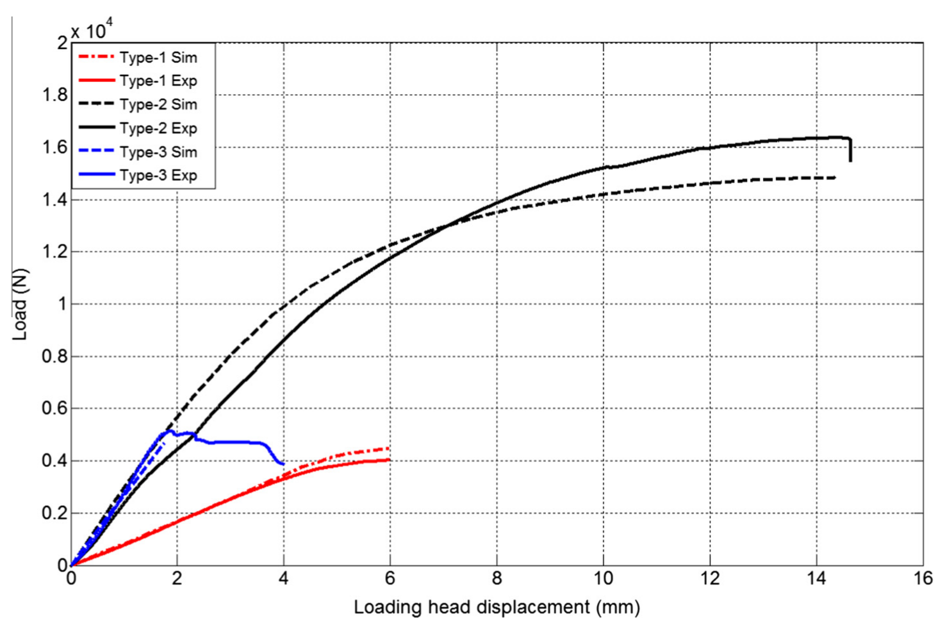

Fig. 15. Comparison between simulation results and experimental data in term of punch force vs. loading head displacement.

flexural loading is investigated. Comparison between simulation results and experimental data in term of punch force versus loading head displacement for three types of sandwich structures before ultimate rupture is illustrated in Fig. 15. In the case of Type-1 and Type-3 sandwich structures, the simulation results matched well with experimental data before ultimate collapse, the deviation in the later stage is due to the buckling and compression failure in laminates and foam core's compression collapse, which needs further investigation. The relatively clear deviation between simulation and experimental results in the case of

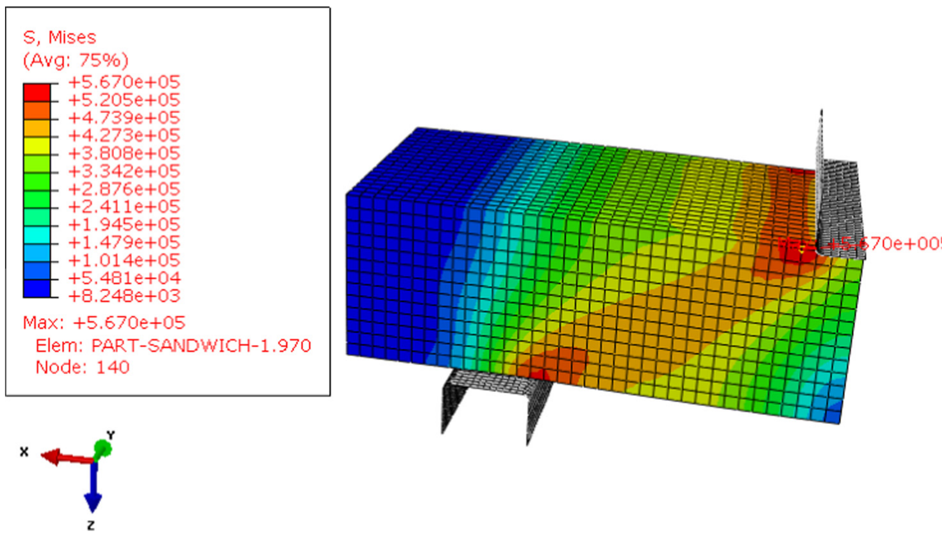

Fig. 16. Von-mises stress contour in PU foam core when the displacement of loading head equals 2.1 mm (Type-1).

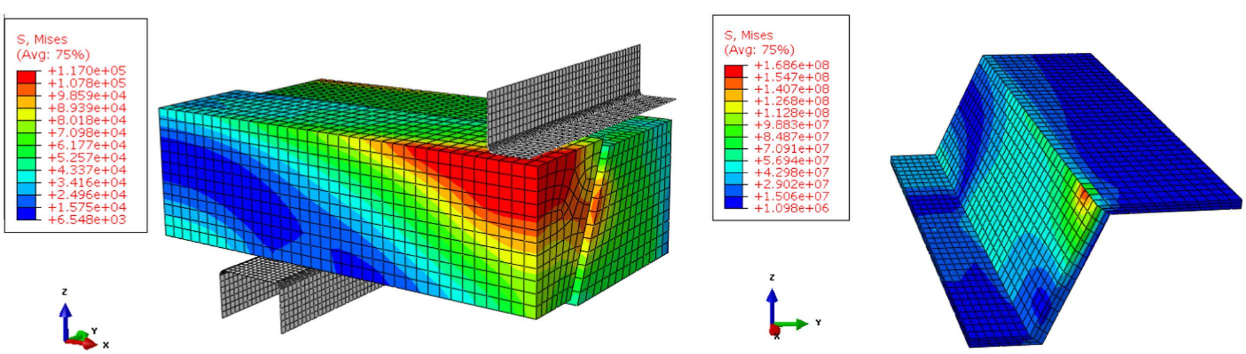

(a) (b)

Fig. 17. Von-mises stress contour when the displacement of loading head equals 2.2 mm (Type-2). Foam core, (b) shear stiffener.

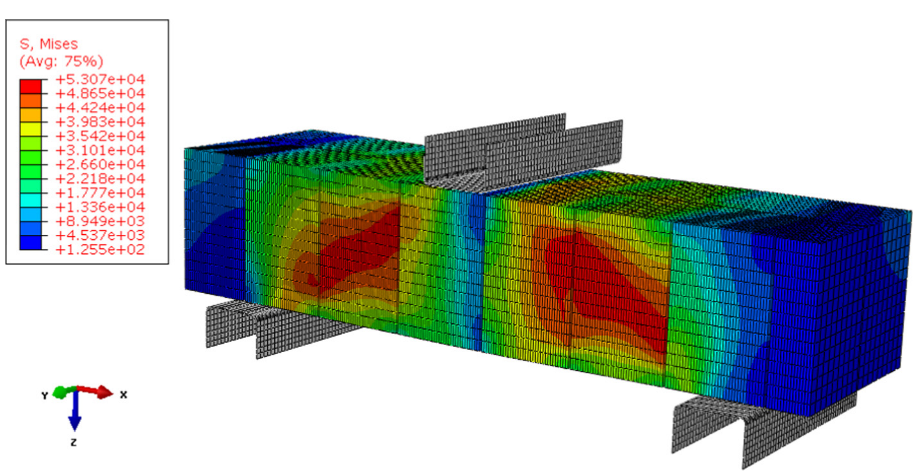

Fig. 18. Von-mises stress contour in the foam core when the displacement of loading head equals 1.75 mm (Type-3).

Type-2 could be due to the simplification of shear stiffener layers and uneven facesheet surface yielded from manufacturing process resulting in the incomplete contact between steel loading head and facesheets. Another reason is the lack of consideration of the progressive damage in composite laminates.

Fig. 16 presents Von-mises stress contour distribution in high density PU foam core when the displacement of loading head equals 2.1 mm. It is found that the maximum Von-mises stress is 0.57 MPa, which is located at the top foam surface near the loading head. Also the maximum compressive stress along *X*-axis S11 on the top most ply of top facesheet is found to be 6.06 MPa, which is much larger than the maximum Von-mises stress in the foam core. Fig. 17 presents Von-mises stress contour in trapezoidal foam core and shear stiffener when the displacement of loading head equals 2.2 mm. It was found that the maximum Von-mises stress is 0.12 MPa for foam core and 168.6 MPa for shear stiffener, which indicates that shear stiffener carries most of loading passing from the punch. Fig. 18 presents Von-mises stress contour distribution in foam core when the displacement of loading head equals 1.75 mm in the case of Type-3 sandwich structure. It is found that the maximum Von-mises stress in foam core is 53.1 kPa, while the maximum compressive stress S22 in the vertical thin stiffener laminates is 98.62 MPa, which indicates the vertical stiffener carries most of loading passing from the punch.

5. Conclusion

Glass fiber/polyurethane sandwich composite structure with three types of foam cores, namely rigid PU foam, prisma foam, and web-core, were successfully manufactured using VARTM process. Performance evaluation of E-glass fiber/PU sandwich composites models was conducted using flexure, flatwise compression and edgewise compression tests to determine the respective stiffness and strength of the models.

Core shear testing of the manufactured sandwich panels proved that Type-2 models have the highest load carrying capacity in bending. In addition, Type-2 model carried the maximum load under flatwise and edgewise compression due to the presence of shear layers. A three-dimensional finite element model was developed for three types of sandwich structures under flexural loading and validated by the experimental results. Based on the experimental results, it is suggested that sandwich panels with prisma cores represent a feasible design for full scale bridge decks. Future work will include the construction of a full scale composite bridge decks using the prisma core and two-part thermoset polyurethane as well as experimental verification of the stresses in the facings and reinforcing laminates (truss).

Acknowledgements

The authors gratefully acknowledge the financial support provided by the Missouri Department of Transportation (MoDOT) and the National University Transportation Center (NUTC) at Missouri University of Science and Technology. The conclusions and opinions expressed in this paper are those of the authors and do not necessarily reflect the official views or policies of the funding institutions. The authors would like to thank Mr. Craig Snyder, Dr. Usama Younes, and Dr. John Hayes from Bayer MaterialScience for their help.

References

[1] Younes U. Development of PU-based RTM and VARTM technology. In: Proceedings of the ACMA composites conference. Las Vegas, NV: 2010. p. 1–17.
[2] Berggreen C, Branner K, Jensen JF, Schultz JP. Application and analysis of sandwich elements in the primary structure of large wind turbine blades. J Sandwich Struct Mater 2007;9:525–52.
[3] Alagusundaramoorthy P, Reddy RVS. Testing and evaluation of GFRP composite deck panels. Ocean Eng 2008;35:287–93.
[4] Manalo AC, Aravinthan T, Karunasena W, Islam MM. Flexural behavior of structural fiber composite sandwich beams in flatwise and edgewise positions. Compos Struct 2010;92:984–95.
[5] Dai J, Hahn HT. Flexural behavior of sandwich beams fabricated by vacuum-assisted resin transfer molding. Compos Struct 2003;61:247–53.
[6] Reisa EM, Rizkalla S. Material characteristics of 3-D FRP sandwich panels. Constr Build Mater 2008;22:1009–18.
[7] Xiong J, Ma L, Wu L, Liu J, Vaziri A. Mechanical behavior and failure of composite pyramidal truss core sandwich columns. Compos B 2011;42:938–45.
[8] Humphreys MF, Erp GV, Tranberg CH. The structural behavior of monocoque fiber composite truss joints. Adv Compos Lett 1999;8(4):173–80.
[9] Canning L, Hollaway L, Thorne AM. Manufacture, testing and numerical analysis of an innovative polymer composite/concrete structural unit. Proc ICE Struct Build 1999;134(3):231–41.
[10] Cartie DD, Fleck NA. The effect of pin reinforcement upon the through-thickness compressive strength of foam-cored sandwich panels. Compos Sci Technol 2003;63:2401–9.
[11] Aref AJ, Alampalli S. Vibration characteristics of a fiber–reinforced polymer bridge superstructure. Des Manuf Compos Struct 2001;52:467–74.
[12] Bitzer T. Honeycomb technology. California: Chapman and Hall; 1997. p. 98–116.
[13] Gibson LJ, Ashby MF. Cellular solids: structure and properties. Cambridge: Cambridge University Press; 1997.
[14] Mohamed M, Vuppalapati RR, Hawkins S, Chandrashekhara K, Schuman T. Impact characterization of polyurethane composites manufactured using vacuum assisted resin transfer molding, Houston: International Mechanical Engineering Congress & Exposition; Texas IMECE2012-88267, 2012, p. 1–8.
[15] Santhanakrishnan R, Dash PK, Stanley AJ, Sabarish M. Flexural property evaluation of GFRP-foam sandwich composite – an experimental approach. ARPN J Eng Appl Sci 2012;7:1300–6.
[16] Corigliano A, Rizzi E, Papa E. Experimental characterization and numerical simulations of a syntactic-foam/glass–fiber composite sandwich. Compos Sci Technol 2000;60:2169–80.
[17] ASTM C364/C364M-07 2007, Standard test method for edgewise compressive strength of sandwich constructions. West Conshohocken, PA: ASTM International; 2007. Available from: <www.astm.org>.